Mycological Progress (2019) 18:771–784
https://doi.org/10.1007/s11557-019-01487-1

DGfM

ORIGINAL ARTICLE

Visiting *Russula* (Russulaceae, Russulales) with samples from southwestern China finds one new subsection of *R.* subg. *Heterophyllidia* with two new species

Jing Wang[1] · Bart Buyck[2] · Xiang-Hua Wang[3] · Tolgor Bau[4]

Received: 16 October 2018 / Revised: 11 March 2019 / Accepted: 14 March 2019

Abstract
Using specimens collected from subtropical pine-fagaceous mixed forests and phylogenetic analysis of DNA sequence data of ITS, 28S rDNA, *rpb2* and *tef1*, we describe two new species, *R. maguanensis* and *R. substriata*, in *R.* subg. *Heterophyllidia*, subsect. *Substriatinae* subsect. nov. *Russula maguanensis* and *R. substriata* are similar to Indian *R. shingbaensis* in the tuberculate-striate pileus and spores with isolated warts but have more vividly coloured pileus and associate with pines and/or fagaceous trees rather than with *Abies*. In our multi-gene phylogeny, the new subsection and a representative of tropical African *R.* subsect. *Aureotactinae* compose one of the four major clades of *R.* subg. *Heterophyllidia*, the three remaining ones corresponding to *R.* sect. *Heterophyllae*, *R.* sect. *Ingratae* and *R.* subsect. *Cyanoxanthinae*. The overall characters of this new section combine those of some other sections in the same subgenus: mostly tuberculate-striate but more vivid pileus, spores with isolated warts, orthochromatic pileipellis with abundant erect aggregate mucronate pileocystidia in the suprapellis but absent in the subpellis and numerous cystidioid hyphae at the bottom of subpellis and trama beneath it. It differs from its sister clade *R.* subsect. *Aureotactinae* in lacking the intense yellowing of surface and context of their fruiting bodies and having pileal cystidioid elements clearly separated by the loose tissue of subpellis from the pileocystidia at the pileus surface. In order to compare our two new species with recently described Asian species and investigate their geographical distributions, we produced an ITS genealogy including also environmental sequences. This ITS genealogy suggests that *R.* subsect. *Substriatinae* includes at least seven potential species, shows an amphi-pacific distribution and its members associate with at least four families of host trees.

Keywords Ectomycorrhizal fungi · Infrageneric classification · Pileipellis · Spores · Taxonomy

Introduction

With the fungal bar-code ITS region being used for identifying specimens and separating species of *Russula* Pers., one of the notoriously difficult groups in the taxonomy of agarics (Singer 1962), Asia is becoming an active region for *Russula* taxonomy. Since the first Chinese *Russula* species supported by ITS data (*R. griseocarnosa* X.H. Wang et al., Wang et al. 2009), 32 new taxa have been described from the country, all primarily based on ITS sequences for species recognition and systematic placement, except for *R. zhejiangensis* G.J. Li et al. with only morphology and *R. vinosobrunneola* G.J. Li & R.L. Zhao on multi-locus data (Li et al. 2011, 2012, 2013a, b, 2015a, b, 2018a, b; Ariyawansa et al. 2015; Zhao et al. 2015; Sang et al. 2016; Das et al. 2017; Jiang et al. 2017a; Tibpromma et al. 2017; Zhang et al. 2017; Li and Deng 2018; Song et al. 2018a, b). In contrast, hardly 13 *Russula* species had been described from China between 1935 and 2009 (Song et al. 2007). In addition, published ITS data confirmed the presence of one Indian (*R. thindii* K. Das & S.L. Miller), one Japanese (*R. subnigricans* Hongo) and 15 European species in China (Yin et al. 2008; Guo et al. 2014; Jiang et al.

Section Editor: Zhu-Liang Yang

✉ Tolgor Bau
junwusuo@126.com

[1] Institute of Mycology, Jilin Agricultural University, Xincheng Avenue 2888, Changchun 130118, People's Republic of China

[2] Institut de Systématique, Ecologie, Biodiversité (ISYEB), Muséum national d'Histoire naturelle, CNRS, Sorbonne Université, case postale 39, 12 rue Buffon, 75013 Paris, France

[3] CAS Key Laboratory for Plant Diversity and Biogeography of East Asia, Kunming Institute of Botany, Chinese Academy of Sciences, Lanhei Road 132, Kunming 650201, People's Republic of China

[4] Institute of Mycology, Jilin Agricultural University, Xincheng Avenue 2888, Changchun 130118, People's Republic of China

2017b; Liu et al. 2017). These ITS-based *Russula* species are found from the northeastern, southern, eastern and southwestern parts of the country, in temperate, subtropical, tropical and subalpine coniferous and broad-leaved forests. Nevertheless, the large number of unnamed sequences from Chinese *Russula* samples in GenBank suggests that the diversity of the genus in China needs further exploring.

During recent forays in subtropical mixed forests dominated by fagaceous trees and *Pinus kesiya* var. *langbianensis* in Maguan County (Wenshan Prefecture, famous for its karst landscape) in Yunnan Province, China, we found several *Russula* specimens for which both morphology and ITS sequences suggested affinities to Indian *R. shingbaensis* K. Das & S.L. Miller. Although ITS sequence data suggested that *R. shingbaensis* belongs to *R.* subg. *Heterophyllidia* Romagn., an exact phylogenetic placement was pending as none of the known sections and subsections within the subgenus seemed appropriate to hold it. Our samples now re-address the problem regarding the phylogenetic placement of *R. shingbaensis* and its sibling *R. verrucospora* Y. Song & L.H. Qiu, recently published from southern China (Song et al. 2018b). Based on the most up to date *Russula* phylogeny using multi-gene data and worldwide sampling (Buyck et al. 2018), we used four loci, the nuc rDNA ITS1-5.8S-ITS2 (ITS), D1-D2 domains of nuc 28S rDNA (28S), part of the second largest subunit of the RNA polymerase II (*rpb2*) (6–7 region) and translation elongation factor 1-alpha (*tef1*) and morphological characters, to (1) delimit the potential new Chinese species from Indian *R. shingbaensis* and Chinese *R. verrucospora*, (2) find a satisfactory infrageneric placement for these Asian species using more conservative loci and (3) find out the distribution area of this species assemblage using all available ITS sequences retrieved from GenBank.

Material and methods

Morphological observation and taxonomic assignment

Descriptions of sporocarps were from fresh material, and micro-morphological study was performed on dried specimens. Basidiospores were observed and measured in Melzer's reagent in side view, excluding ornamentation and apiculus. For each fruiting body, 20 spores were measured. All other micro-morphological structures were revived in 5% KOH then mounted with Congo red (aqueous solution). Pileipellis was examined for the presence of ortho- or metachromatic contents in Cresyl blue (aqueous solution) as explained in Buyck (1989). Sulphovanillin (SV) was used to test the reactions of cystidium contents. All drawings except those of the basidiospores were made with the aid of a drawing tube installed on a Nikon E400 microscope. Vertical sections of the pileipellis were cut approximately at the mid-radius of the pileus. Sections through the stipitipellis were taken from the middle part along the stipe length. Drawings of basidiospores were made by hand, using a 5000× amplification (1 cm on paper standing for 2 μm). The abbreviation for spore measurements (*n/m/p*) means *n* spores from *m* basidiocarps of *p* specimens. Measurements (and Q values) of spores are given as (a) b–***m***–c (d), in which "a" is the lowest value, "d" the biggest, "***m***" the mean and "b–c" covers a minimum of 90% of the values. "Q" stands for the ratio of length and width of a spore and "***Q*** ± av" for the average Q of all spores ± sample standard deviation. Colour codes of fruiting bodies are from Kornerup and Wanscher (1961). Voucher specimens are deposited in Cryptogamic Herbarium, Kunming Institute of Botany, Chinese Academy of Sciences (HKAS section, KUN). Infrageneric classification follows Buyck et al. (2018).

DNA extraction, PCR amplifications and sequencing

DNA extraction and PCR protocols followed Wang et al. (2015). The following four regions were amplified: complete ITS (c. 700 bp), 28S (c. 900 bp), *rpb2* (c. 800 bp) and *tef1* (c. 920 bp). Primer pairs ITS1F + ITS4 or ITS5 + ITS4, LROR+ LR5 and RPB2-6F + fRPB2-7cR were used to amplify the ITS, 28S and *rpb2* regions/genes, respectively (Vilgalys and Hester 1990; White et al. 1990; Liu et al. 1999; Moncalvo et al. 2000). The *tef1* gene was amplified in two pieces using the primer combinations 526F + EF-ir and 983F + 1567R (Rehner and Buckley 2005; Hansen et al. 2013). For problematic samples where the 526F–EF-ir region did not successfully amplify, a newly designed specific reverse primer EF-ir-Subs (5′-GAAATGCCTGCCTCGAATTCACC-3′) was used with the forward primer 526F. PCR products were visualised via UV light after electrophoresis on 1% agarose gels stained with ethidium bromide. Successful PCR products were sent to Sangon Biotech Limited Company (Shanghai, China) for Sanger sequencing using the same primers as PCR. When sequences have heterozygous INDELs or ambiguous sites, samples were sequenced bidirectionally to make contigs of the amplified regions or verify the ambiguous sites. Raw sequences were assembled with Sequencher v4.1.4 (Gene Codes Corporation, Ann Arbor, USA), and assembled sequences are deposited in GenBank (Table 1, Fig. 2).

Taxa sampling and phylogenetic analyses of multi-gene data

All our samples were sequenced to obtain 28S, *rpb2* and *tef1* sequences. Besides our two species with 18 sequences, 55 species (with at least two of the three loci available) were selected to cover all the seven subgenera of *Russula* recognised by Buyck et al. (2018) and major clades in Looney et al. (2016). Specifically, representative species of

Table 1 Taxa and collections used for multi-gene phylogenetic analyses in this study. Sequences produced in the present study are in bold. The other sequences are from Buyck et al. (2018) except those of *R. aeruginea*, *R. cyanoxantha*, *R. heterophylla*, *R. ochrospora* and *R. parazurea* from Buyck et al. (2008) and *R. compacta*, *R.* cf. *pseudolepida* and *R. variata* from Looney et al. (2016). 28S = 28S rDNA, *rpb2* = part of the second largest subunit of the RNA polymerase II (6–7 region), *tef1* = translation elongation factor 1-alpha

Species	Geographical origin	Specimen voucher	GenBank accession		
			28S	*rpb2*	*tef1*
Lactifluus allardii	USA	B. Buyck 07.141	KU237532	KU237818	KU237962
L. aff. *volemus*	USA	B. Buyck 07.048	KU237574	KU237860	KU238002
R. adusta	Canada	B. Buyck 06.562	KU237476	KU237762	KU237907
R. aeruginea	Sweden	AT2003017	DQ421999	DQ421946	–
R. albonigra	Slovakia	B. Buyck 07.291	KU237536	KU237822	KU237966
R. amoenolens	Italy	B. Buyck 08.675	KU237562	KU237848	–
R. cf. *annulata*	Madagascar	B. Buyck 06.048	KU237470	KU237756	KU237902
R. archaeosuberis	Italy	B. Buyck 12.085	KU237593	KU237878	KU238019
R. aff. *areolata*	Madagascar	B. Buyck 06.090	KU237471	KU237757	KU237903
R. aff. *brunneoannulata*	Madagascar	B. Buyck 06.029	KU237452	KU237738	KU237887
R. camarophylla	Spain	M.P. de Gregorio 11.7.09	KU237579	KU237865	KU238006
R. cf. *cellulata*	Madagascar	B. Buyck 06.045	KU237454	KU237740	KU237889
R. compacta	USA	D.P. Lewis 242	KT933819	KT933890	–
R. aff. *crustosa*	Canada	B. Buyck 06.616	KU237461	KU237747	KU237896
R. cyanoxantha	France	U. Eberhardt 29.09.2002–2	DQ422033	DQ421970	–
R. aff. *delica*	Italy	B. Buyck 12.086	KU237594	KU237879	KU238020
R. edulis	Madagascar	B. Buyck 08.167	KU237564	KU237850	KU237993
R. elastica	Madagascar	B. Buyck 06.009	KU237451	KU237737	–
R. emetica	France	J.M. Trendel 39.08092228	KU237578	KU237864	–
R. farinipes	Italy	B. Buyck 08.632	KU237561	KU237847	KU237992
R. fellea	Slovakia	B. Buyck 07.281	KU237507	KU237793	KU237936
R. fistulosinae sp. ined.	Madagascar	B. Buyck 08.105	KU237527	KU237813	KU237957
R. flavobrunnea var. *violaceotincta*	Madagascar	B. Buyck 06.050	KU237468	KU237754	KU237901
R. gossypina	Madagascar	B. Buyck 06.002	KU237450	KU237736	KU237886
R. grisea	Slovakia	B. Buyck 07.184	KU237509	KU237795	KU237939
R. aff. *griseobrunnea*	New Caledonia	B. Buyck 09.344	KU237592	KU237877	KU238018
R. herrerae	Mexico	B. Buyck 06.532	KU237486	KU237772	KU237915
R. heterophylla	Sweden	U. Eberhardt 20.08.2004–2	DQ422006	–	DQ421951
R. ilicis	Italy	M. Floriani 00.300	KU237595	KU237880	KU238021
R. cf. *illota*	Mexico	B. Buyck 06.380	KU237464	KU237750	KU237898
R. integra	Estonia	B. Buyck 07.198	KX812899	KU237799	KU237943
R. ionochlora	France	B. Buyck 07.338	KU237508	KU237794	KU237938
R. aff. *laurocerasi*	Mexico	B. Buyck 06.610	KU237458	KU237744	KU237893
R. langei	France	B. Buyck 07.792	KU237510	KU237796	KU237940
R. lepida	Slovakia	B. Buyck 07.189	KU237500	KU237786	KU237930
R. madecassensis	Madagascar	B. Buyck 06.146	KU237456	KU237742	KU237891
R. aff. *madecassensis*	Madagascar	B. Buyck 06.255	KU237475	KU237761	KU237906
R. maguanensis	China	X.H. Wang 4765	**MH714537**	**MH939989**	**MH939983**
R. mariae	USA	B. Buyck 07.038	KU237538	KU237824	KU237968
R. medullata	Slovakia	B. Buyck 07.252	KU237546	KU237832	KU237976
R. mustelina	Slovakia	S. Adamcik 09.88	KU237596	KU237881	KU238022
R. ochrospora	Italy	G. Donelli 20.07.2004	DQ422012	DQ421953	–
R. oleifera	Burundi	B. Buyck 98.024	KU237490	KU237776	KU237919
R. ornaticeps	Canada	B. Buyck 06.530	KU237466	KU237752	–

Table 1 (continued)

Species	Geographical origin	Specimen voucher	GenBank accession		
			28S	*rpb2*	*tef1*
R. aff. *pallidospora*	Spain	M.P. Gregorio 13.6.08	KU237580	KU237866	KU238007
R. parazurea	Italy	M. Floriani 01.10.2003	DQ422007	DQ421945	–
R. polyphylla	USA	B. Buyck 07.134	KP033497	KP033508	KU238023
R. polyphyllinae sp. ined.	USA	B. Buyck 09.215	KU237590	KU237875	–
R. prolifica	Madagascar	B. Buyck 06.161	KU237455	KU237741	KU237890
R. pseudocarmesina	Madagascar	B. Buyck 06.030	KU237453	KU237739	–
R. pseudociliata	Madagascar	B. Buyck 08.061	KU237537	KU237823	KU237967
R. cf. *pseudolepida*	USA	B. P. Lewis 247	KT933821	KT933892	–
R. pulverulenta	USA	B. Buyck 05.160	KU237563	KU237849	–
R. cf. *roseoalba*	Madagascar	B. Buyck 06.105	KU237472	KU237758	–
R. substriata	China	J. Wang 292	**MH714538**	**MH939990**	**MH939984**
R. substriata	China	X.H. Wang 4749	**MH714539**	**MH939991**	**MH939985**
R. substriata	China	X.H. Wang 4766	**MH714540**	**MH939992**	**MH939986**
R. substriata	China	X.H. Wang 4767	**MH714541**	**MH939993**	**MH939987**
R. substriata	China	X.H. Wang 4785	**MH714542**	**MH939994**	**MH939988**
R. variata	USA	B.P. Lewis 241	KT933818	KT933889	–
R. cf. *vesca*	Mexico	B. Buyck 06.525	KU237465	KU237751	KU237899
R. violeipes	Slovakia	B. Buyck 07.273	KU237534	KU237820	KU237964
R. aff. *virescens*	New Caledonia	B. Buyck 09.021	KU237582	KU237868	KU238009

the various recognised subdivisions of *R.* subg. *Heterophyllidia* (in which the target group of this study is placed) used by Buyck et al. (2018) were included. These sequences formed a 28S-*rpb2*-*tef1* combined dataset, which was used to determine the phylogenetic position of our two new species. *Lactifluus* aff. *volemus* and *L. allardii* were chosen as outgroup, following the phylogeny of Russulaceae of Buyck et al. (2008).

Alignments were made using the online version of the multiple sequence alignment program MAFFT v7 (Katoh and Toh 2008), applying the L-INS-I strategy, and were manually adjusted in BioEdit v.7.1.3.0 (Hall 1999). Introns of *rpb2* and *tef1* and an ambiguous section of *rpb2* (ca 550 bp from the RPB2-6F primer) were removed from phylogenetic analyses. We followed the partitioning strategy of Buyck et al. (2018), i.e., seven partitions (28S, *rpb2* 1st, *rpb2* 2nd, *rpb2* 3rd codons, *tef1* 1st, *tef1* 2nd and *tef1* 3rd codons) as this partition gave higher bootstrap proportions (BP) in the maximum likelihood (ML) analysis of multi-gene phylogeny of the whole genus. ML phylogenetic analysis was conducted in RAxML v7.2x (Stamatakis 2006) and Bayesian inference (BI) in MrBayes v3.2.6 (Ronquist et al. 2012). ML analysis was executed applying the rapid bootstrap algorithm with 1000 replicates, followed by a ML tree search. For BI analysis, the best-fit model was selected by MrModeltest (Nylander 2004). The BI analysis was conducted using four runs with four chains each for one million generations sampling every 100th tree. Runs were inspected to make sure the average standard deviation of split frequencies went below 0.01 and effective sampling sizes were > 200 in Tracer v1.7.0 (Rambaut et al. 2018). A 50% majority rule consensus tree was built after discarding trees from a 25% burn-in. A ML-BP ≥ 70% and BI posterior probability (BI-PP) ≥ 95% were considered as significant support for a node to be monophyletic. The most likely tree generated in ML was viewed and exported in FigTree v1.3.1, with BI-PP added on the corresponding nodes. Matrix and the ML and BI trees are deposited in TreeBASE as study ID S23424.

Taxa sampling and phylogenetic analyses of ITS data

The six generated ITS sequences from our six samples (with the 18S and 28S ends trimmed) were submitted to BLASTn to find matches with high similarity (≥ 90%) and query cover (> 90%) in GenBank. The complete ITS, ITS1 and ITS2 were submitted, respectively, to retrieve sequences with different sizes. We retrieved sequences both from fruiting bodies and environmental samples to find out whether representatives of our new species and section have been recorded from other places. Following the phylogenetic implication of the 28S-*rpb2*-*tef1* data, we included four ITS sequences of the *R. brunneoannulata* Buyck species complex. To show the genetic diversification among the two new species and some representative species or look-alikes in the same subgenus,

especially those originally described from Asia and Africa, we included 61 ITS sequences of 38 species. Among these species, seven are from Europe. The purpose of including these European species is to indicate the traditional taxonomic classification, which is mostly based on European representatives. The ITS data were analysed to show how the two new species differ genetically from their relatives, the geographical distribution of the new section and the two new species and their putative hosts. We used four species of *R.* subg. *Compactae* (Fr.) Bon and *R.* subg. *Archaea* Buyck & V. Hofst. as outgroups, following the phylogeny of Buyck et al. (2018). The 18S and 28S ends of the ITS sequences were removed from phylogenetic analyses. Aligning and further analyses of the ITS data followed those of the 28S-*rpb2-tef1* dataset, except that no partitioning was set and 200 million generations were ran for BI analysis. A ML-BP ≥ 70% and BI-PP ≥ 95% were considered as significant support for a node to be monophyletic. Matrix and the ML and BI trees are deposited in TreeBASE with study ID S23424, the same as *28S-rpb2-tef1* dataset.

Results

Multigene phylogeny

For BI analysis, GTR + I + G model was selected as the best-fit model by MrModeltest. ML and BI analyses of the 28S-*rpb2-tef1* combined dataset produced nearly identical topologies with comparable support values (Fig. 1). Except that in the BI analysis the remaining of *Russula* excluding *R.* subg. *Heterophyllidia* was significantly supported to be a monophyly (BI-PP 0.97), the two analyses did not resolve the relationships among the major clades/subgenera of *Russula*. Nevertheless, except for *R.* subg. *Crassotunicata* Buyck & V. Hofst. (a singleton of *R. farinipes* Romell), all the subgenera were retrieved with high supports (ML-BP 89–100%, BI-PP 1.00). The six samples of the two new species formed a highly supported terminal clade with ML-BP 100% and BI-PP 1.00 with a long branch, sister to a singleton also with a long branch formed by African *R.* aff. *brunneoannulata* with ML-BP 71% and BI-PP 0.98. This Asian-African clade (clade B, Fig. 1) represented one of the four highly supported major clades of *R.* subg. *Heterophyllidia* (clades A–D). The phylogenetic relationships among these four clades did not receive supports either in the ML or BI analysis.

ITS genealogy

The aligned ITS dataset includes 96 sequences and 811 characters (with the 18S and 28S ends trimmed), 311 bp of ITS-1, 156 bp of 5.8S and 343 bp of ITS-2. All sequences cover ITS-1, 5.8S and ITS-2 regions, except for AB509486 and AB509982 lacking ITS-1 region. ML analysis produced a genealogy without support for relationships among the six significantly supported major clades of the ingroup (clades A–F, Fig. 2). For BI analysis, HKY + I + G model was selected as the best-fit model by MrModeltest. BI analysis produced a highly similar typology with most supports comparable to the ML analysis. The only two differences between the two analyses are on the branch leading to the terminal clade formed by HKAS 102275, 102278 and 102279, which received significant support only in the ML analysis (ML-BP 85%) and two basal branches of clade F, which received significant supports only in the BI analysis (BI-PP 0.98 and 0.99). Our six samples from Maguan fell into one of the six major clades, clade A (ML-BP 100%, BI-PP 1.00) together with 21 mostly environmental samples from Australia, China, India, Japan, Malaysia, Mexico and USA which can be assigned into three additional highly supported subclades and two singletons. One of the singletons is the holotype of *R. shingbaensis* from India and the other a Malaysian sample (from Bornean island). In general, clade A shows an amphi-pacific distribution pattern and hosts of this clade involve Pinaceae (*Abies* and *Pinus*), Fagaceae (*Castanopsis* and *Quercus*), Jaglandaceae (*Oreomunnea*) and Myrtaceae (*Eucalyptus*). The assemblage of clade A is the new subsection we describe below. Within clade A, our five samples, together with five samples from eastern (Zhejiang), central-southern (Hunan) and southwestern (Sichuan) China, and two samples from central and southern Japan formed a fully supported terminal clade. Our last sample HKAS 102277 and a sample also from southern Japan formed another highly supported terminal clade with ML-BP 99% and BI-PP 1.00. These two terminal clades are the two new species that are described in this study.

The successive clades of clade A are clade B, represented by a single species *R. verrucospora* and then a superclade formed by clade D (*R.* cf. *brunneoannulata*) and C (*R.* subsect. *Cyanoxanthinae* Singer). These sibling relationships, however, are without support in either analysis. *Russula verrucospora* was shown to be a sister of *R. shingbaensis* by Song et al. (2018b) with ML-BP 84% and *R.* cf. *brunneoannulata* was sibling to the clade formed by our two new species in the 28S-*rpb2-tef1* phylogeny. Both species have spores with isolated warts and numerous pileocystidia and gloeoplerous elements in all tissues. The remaining two clades E and F are well in line with those in the 28S-*rpb2-tef1* phylogeny, i.e. corresponding to *R.* sect. *Heteropyllae* Fr. and *R.* sect. *Ingratae* (Quél.) Maire in the infrageneric classification of *Russula.*

Taxonomy

Russula maguanensis J. Wang, X.H. Wang, Buyck & T. Bau, sp. nov., Figs. 3a and 4.

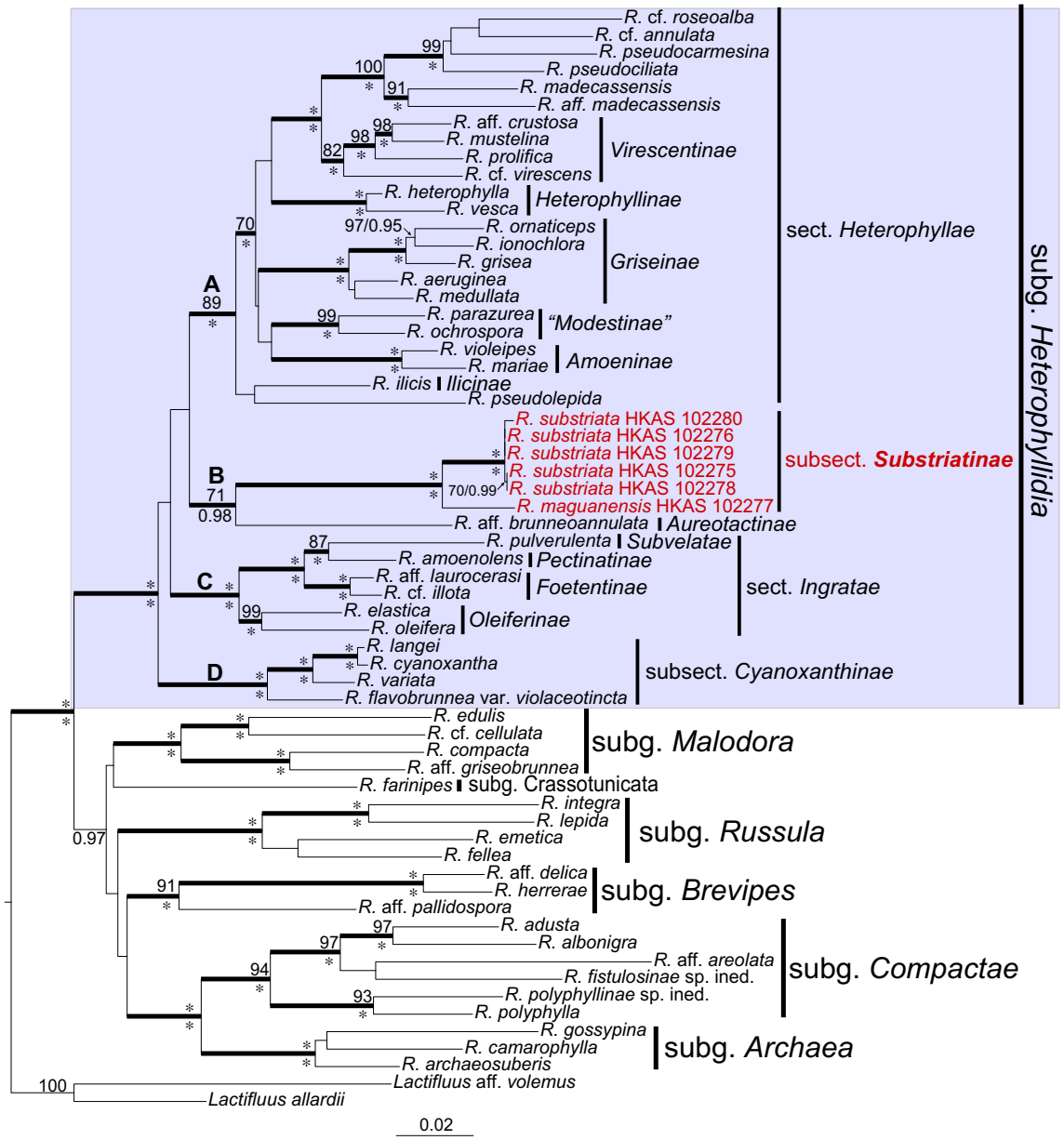

Fig. 1 Most likely tree generated by maximum likelihood (ML) analysis of *Russula* species using 28S, *rpb2* and *tef1* sequence data (2299 bp), rooted with *Lactifluus* aff. *volemus* and *L. allardii*. Greyish-blue frame indicates the subgenus where the two new species *R. maguanensis* and *R. substriata* and the new subsection *R.* subsect. *Substriatinae* (in red) are placed. Infrageneric classification follows Buyck et al. (2018). Names of the infrageneric taxa under *R.* sect. *Ingratae* and *R.* sect. *Heterophyllae* are all of subsections except for *Subvelatae* of a section. We put the name *Modestinae* in quotation marks because the type specimen of *R. modesta* does not correspond to the current concept of the species. ML bootstrap values (ML-BP) and Bayesian posterior probabilities (BI-PP) are shown above and below the branches respectively. A ML-BP 100% or BI-PP 1.0 is replaced by an asterisk (*). Branches supported by both ML-BP ≥ 70% and BI-PP ≥ 95% are in black bold

MycoBank: MB 827272.

GenBank: MH724918 (ITS), MH714537 (28S), MH939989 (*rpb2*), MH939983 (*tef1*), all from holotype.

Etymology: named after Maguan County, the type locality.

Holotype: China, Yunnan Prov., Wenshan Pref., Maguan Co., Dalishu Town, Xiangchang, 23°04′07.6″ N, 104°12′31.5″ E, 1633 m asl, in mixed forest of fagaceous trees and *Pinus kesiya* var. *langbianensis*, leg. X.H. Wang, 14 Oct. 2017, no. 4765 (HKAS 102277, KUN!).

Diagnosis: A species with medium-sized basidiocarps, sticky tuberculate-striate pileus with lilac red tinge, finely to coarsely cracked pileus cuticle, spores with isolated warts and suprapellis with tufts of pileocystidia.

Pileus 27–45 mm diam., concave with applanate margin, almost flat in the extreme centre, 60–70% of the radius strongly tuberculate-striate; surface finely cracked even when humid, reddish lilac to lilac (14B5-15B5), rapidly purplish white to purplish pink (close to 14A2 and 14A3) towards the margin

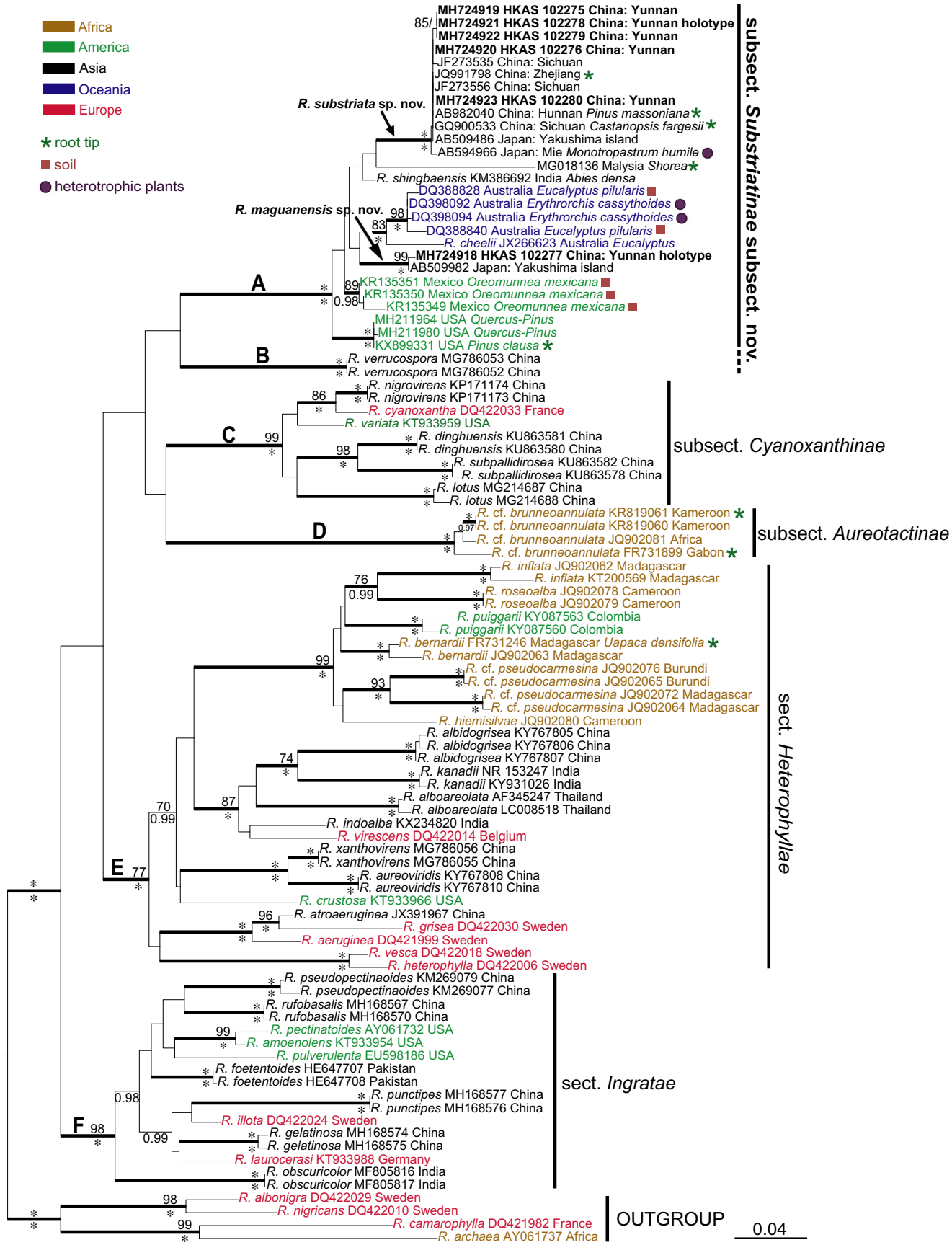
Africa
America
Asia
Oceania
Europe
root tip
soil
heterotrophic plants
R. substriata sp. nov.
R. maguanensis sp. nov.
MH724919 HKAS 102275 China: Yunnan
MH724921 HKAS 102278 China: Yunnan holotype
MH724922 HKAS 102279 China: Yunnan
MH724920 HKAS 102276 China: Yunnan
JF273535 China: Sichuan
JQ991798 China: Zhejiang
JF273556 China: Sichuan
MH724923 HKAS 102280 China: Yunnan
AB982040 China: Hunnan Pinus massoniana
GQ900533 China: Sichuan Castanopsis fargesii
AB509486 Japan: Yakushima island
AB594966 Japan: Mie Monotropastrum humile
MG018136 Malysia Shorea
R. shingbaensis KM386692 India Abies densa
DQ388828 Australia Eucalyptus pilularis
DQ398092 Australia Erythrorchis cassythoides
DQ398094 Australia Erythrorchis cassythoides
DQ388840 Australia Eucalyptus pilularis
R. cheelii JX266623 Australia Eucalyptus
MH724918 HKAS 102277 China: Yunnan holotype
AB509982 Japan: Yakushima island
KR135351 Mexico Oreomunnea mexicana
KR135350 Mexico Oreomunnea mexicana
KR135349 Mexico Oreomunnea mexicana
MH211964 USA Quercus-Pinus
MH211980 USA Quercus-Pinus
KX899331 USA Pinus clausa
R. verrucospora MG786053 China
R. verrucospora MG786052 China
R. nigrovirens KP171174 China
R. nigrovirens KP171173 China
R. cyanoxantha DQ422033 France
R. variata KT933959 USA
R. dinghuensis KU863581 China
R. dinghuensis KU863580 China
R. subpallidirosea KU863582 China
R. subpallidirosea KU863578 China
R. lotus MG214687 China
R. lotus MG214688 China
R. cf. brunneoannulata KR819061 Kameroon
R. cf. brunneoannulata KR819060 Kameroon
R. cf. brunneoannulata JQ902081 Africa
R. cf. brunneoannulata FR731899 Gabon
R. inflata JQ902062 Madagascar
R. inflata KT200569 Madagascar
R. roseoalba JQ902078 Cameroon
R. roseoalba JQ902079 Cameroon
R. puiggarii KY087563 Colombia
R. puiggarii KY087560 Colombia
R. bernardii FR731246 Madagascar Uapaca densifolia
R. bernardii JQ902063 Madagascar
R. cf. pseudocarmesina JQ902076 Burundi
R. cf. pseudocarmesina JQ902065 Burundi
R. cf. pseudocarmesina JQ902072 Madagascar
R. cf. pseudocarmesina JQ902064 Madagascar
R. hiemisilvae JQ902080 Cameroon
R. albidogrisea KY767805 China
R. albidogrisea KY767806 China
R. albidogrisea KY767807 China
R. kanadii NR 153247 India
R. kanadii KY931026 India
R. alboareolata AF345247 Thailand
R. alboareolata LC008518 Thailand
R. indoalba KX234820 India
R. virescens DQ422014 Belgium
R. xanthovirens MG786056 China
R. xanthovirens MG786055 China
R. aureoviridis KY767808 China
R. aureoviridis KY767810 China
R. crustosa KT933966 USA
R. atroaeruginea JX391967 China
R. grisea DQ422030 Sweden
R. aeruginea DQ421999 Sweden
R. vesca DQ422018 Sweden
R. heterophylla DQ422006 Sweden
R. pseudopectinaoides KM269079 China
R. pseudopectinaoides KM269077 China
R. rufobasalis MH168567 China
R. rufobasalis MH168570 China
R. pectinatoides AY061732 USA
R. amoenolens KT933954 USA
R. pulverulenta EU598186 USA
R. foetentoides HE647707 Pakistan
R. foetentoides HE647708 Pakistan
R. punctipes MH168577 China
R. punctipes MH168576 China
R. illota DQ422024 Sweden
R. gelatinosa MH168574 China
R. gelatinosa MH168575 China
R. laurocerasi KT933988 Germany
R. obscuricolor MF805816 India
R. obscuricolor MF805817 India
R. albonigra DQ422029 Sweden
R. nigricans DQ422010 Sweden
R. camarophylla DQ421982 France
R. archaea AY061737 Africa
A
B
C
D
E
F
subsect. Substriatinae subsect. nov.
subsect. Cyanoxanthinae
subsect. Aureotactinae
sect. Heterophyllae
sect. Ingratae
OUTGROUP
0.04

◀ **Fig. 2** Most likely tree generated by maximum likelihood (ML) analysis of *Russula* species using ITS sequence data (811 bp), rooted with four species of *R.* subg. *Compactae* (outgroup). Infrageneric classification follows Buyck et al. (2018). Sample names are provided in the order of species name (if available), GenBank accession number, origin of country and host (if available). For the sequences generated in this study, herbarium number is provided after the GenBank accession. For the two new species described, province name is provided after its country. ML bootstrap values (ML-BP) and Bayesian posterior probabilities (BI-PP) are shown above and below the branches, respectively. A ML-BP 100% or BI-PP 1.0 is replaced by an asterisk (*). Branches supported by both ML-BP ≥ 70% and BI-PP ≥ 95% are in black bold. Dashed part of the bar for *R.* subsect. *Substriatinae* indicates the uncertainty of the placement of *R. verrucospora* in the subsection

and in the extreme centre, slimy-glutinous when wet, cuticle nearly completely separable. Stipe 30–45 × 7–7.5 mm, central, cylindrical, uniformly white, stuffed-spongy inside. Lamellae adnate, equal or with occasional lamellulae, 3–3.5 mm high, medium-crowded, strongly anastomosing in between and towards the stipe attachment, brittle, cream white. Context white, 1 mm thick in the pileus. Taste acrid. Odour none. Spore print not obtained.

Basidiospores (60/3/1/) (7.5) 8.0–***8.5***–9.5 × (6.5) 7.0–***7.4***–8.0 (8.5) μm [Q = (1.06) 1.08–1.23 (1.25), **Q = *1.15* ± 0.04**], subglobose to broadly ellipsoid; ornamentation amyloid, 0.5–1.5 μm high, composed of isolated warts never fused, conical or blunt, rarely truncate at the apex, 0.3–1.0 μm in diam.; suprahilar plage inamyloid, rarely slightly distally amyloid. Basidia 30–50 (60) × 9–15 μm, subclavate, 4-spored. Gloeocystidia common on sides and edges of the gills, 45–80 × 9–14 μm on sides, 32–52 × 7–12 μm on edges, mostly buried among the basidia, some projecting up to 20 μm beyond the basidia-layer on sides, fusiform, rarely lanceolate, often mucronate or even moniliform at the apex, with dense granular or crystalline contents turning to blackish grey in SV. Marginal cells not differentiated. Lamellar trama composed of rosettes and connective hyphae, sphaerocytes 15–30 μm in diam., connective hyphae 2–5 μm wide. Pileipellis orthochromatic in Cresyl blue, two-layered, covered with sparse slime, 500–800 μm thick, with a distinctly delimited suprapellis sitting on a well-delimited and strongly gelatinized subpellis of narrow hyphae that is abruptly separated from the voluminous sphaerocystes of trama; suprapellis a trichoderm, 50–70 μm thick, of abundant pileocystidia and inflated, septate, poorly branching, hyphal extremities composed of 1–4 cells 4–10 (12) μm wide, the terminal cells up to 37 μm long, usually tapering; pileocystidia (23) 30–60 × 5–10 μm, fusiform, sublanceolate, often mucronate or with a central knob at the apex, with strongly refractive granular or crystalline contents turning to greyish black or dark brown in SV; subpellis a loose tissue of very narrow hyphae lacking pileocystidia, 450–750 μm thick, hyphae 2–3 μm wide, hyaline, with clear outline in a

Fig. 3 Basidiocarps. **a** *Russula maguanensis* (HKAS 102277, holotype). **b**–**d** *R. substriata*: **b** HKAS 102278 (holotype), **c** HKAS 102276, **d** HKAS 102280. Bar: 1 cm

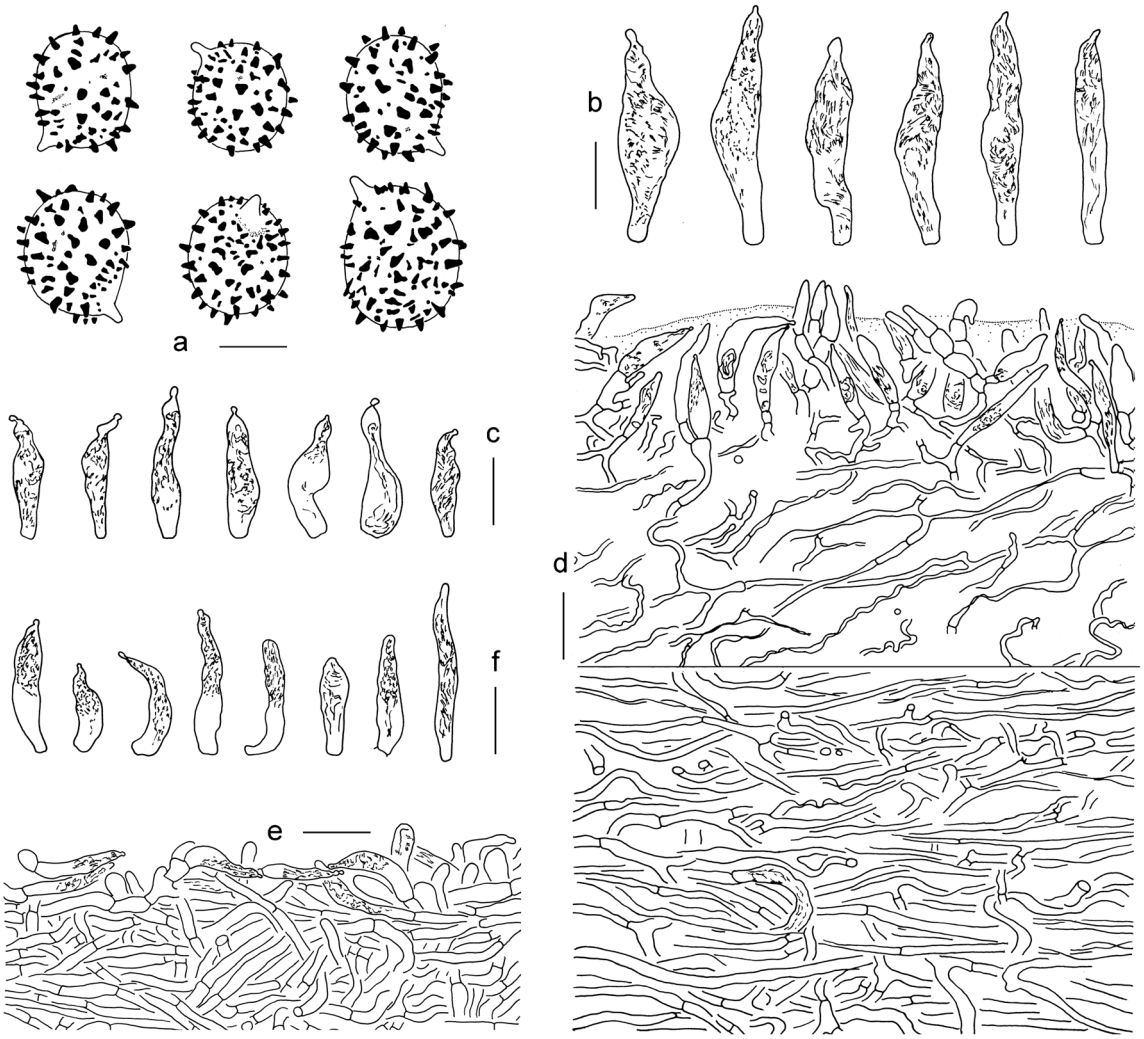

Fig. 4 *Russula maguanensis* (HKAS 102277, holotype). **a** Basidiospores. **b** Gloeocystidia on gill sides. **c** Gloeocystidia on gill edges. **d** Pileipellis. **e** Stipitipellis. **f** Caulocystidia. Bars: **a** 5 μm; **b**, **c**, **f** 20 μm; **d**, **e** 25 μm

gelatinized matrix, often branching, becoming repent and slightly wider (up to 4 μm) towards pileus trama, at the very bottom and adjacent trama with scattered to moderately numerous cylindrical cystidioid hyphae 80–260 × 7–13 μm, those with strongly refractive crystalline contents turning to greyish black in SV. Stipitipellis one-layered, 30–60 μm thick; caulocystidia common, 25–44 × 5–7 μm, fusiform, rarely sublanceolate or subcylindrical, with crystalline contents changing to greyish black in SV. Pileus and stipe trama with numerous rosettes and connective hyphae; sphaerocystes 13–70 μm in diam, connective hyphae 3–8 μm wide. Clamp connections absent.

Habit, habitat and distribution Scattered, during fall, in mixed forest of fagaceous trees and *Pinus kesiya* var. *langbianensis*. Southwestern China and Japan (Mie, Yakushima Island).

Notes: Because of the pronounced, areolate-squamulose aspect of the pileus surface, our species is similar to those of *R.* subg. *Heterophyllidia* subsect. *Virescentinae* Singer, particularly those in the *R. crustosa* Peck complex and species in *R.* subsect. *Aureotactinae* R. Heim ex Buyck. When considering in addition the vividly coloured pileus with tuberculate-striate margin, our species could also easily be confused with some tropical African *Heterophyllinae* near *R. roseoviolacea* Buyck. Those African species, however, all have subreticulate to reticulate spores (Buyck 1994). For more notes, see under *R. substriata* and Discussion.

Russula substriata J. Wang, X.H. Wang, Buyck & T. Bau, sp. nov., Figs. 3b–d and 5.

MycoBank: MB 827273.

GenBank: MH724921 (ITS), MH714540 (28S), MH939992 (*rpb2*), MH939986 (*tef1*), all from holotype.

Etymology: named after the striate pileus.

Holotype: China, Yunnan Prov., Wenshan Pref., Maguan Co., Dalishu Town, Xiangchang, 23°03′59.28″ N, 104°12′41.31″ E, 1656 m asl, in mixed forest of fagaceous trees and *Pinus kesiya* var. *langbianensis*, leg. X.H. Wang, 14 Oct. 2017, no. 4766 (HKAS 102278, KUN!).

Diagnosis: A medium-sized species recognised by the sticky tuberculate-striate pileus with greyish rose tinge, finely to coarsely cracked pileus cuticle, spores with isolated warts and outmost pileipellis with aggregate pileocystidia.

Pileus 30–50 mm diam., hemispherical at first, later convex, finally concave with applanate margin, 50–70% of the radius strongly tuberculate-striate, finely to coarsely cracked even when humid, slimy-glutinous when wet, cuticle completely separable, greyish rose (11B3, 12B3), often much darker at the centre, margin cream-white or pinkish white (12A2) in age. Context of pileus 1–2 mm thick, white. Stipe 35–65 × 6–12 mm, central, equal or tapering upwards, with 6–10 cavities inside, neither extremely fragile nor very hard, cream white at the upper part, with purple-pinkish or pinkish tinge at the low part, finely scaly near base. Lamellae 2–6 mm high, much broader than flesh thickness, adnate, slightly attenuate towards pileus margin, medium-crowded (13–14 L/cm), shorter lamellulae not frequent to common, strongly anastomosing towards flesh, sometimes anastomosing and forming zone around stipe, elastic and greasy-buttery, cream white. Odour reminiscent of *R. foetens*. Taste mild. Spore print not obtained.

Basidiospores (200/10/5) 8.0–***9.0***–10.0 (11.0) × (6.5) 7.0–***7.5***–8.0 (9.0) μm [Q = (1.03) 1.11–1.30 (1.36), **Q = *1.20*** ± 0.06], broadly ellipsoid to ellipsoid, ornamentation amyloid, 0.5–1.8 μm high, composed of isolated warts with conical, round or truncate apex, suprahilar plage inamyloid. Basidia 28–63 × 11–16 μm, subclavate, 4-spored. Gloeocystidia common to numerous on sides and edges of the gills, 38–80 × 9–15 μm on sides, 23–45 × 6–11 μm on edges, mostly buried among the basidia, fusiform, mucronate or moniliform at the apex, with dense granular, crystalline or amorphous contents blackish grey in SV. Marginal cells not differentiated. Lamellar trama composed of rosettes and connective hyphae, sphaerocystes 8–50 μm in diam., connective hyphae 3–5 μm wide, oleiferous hyphae common, 5–9 μm wide, with granular contents. Pileipellis orthochromatic in Cresyl blue, mostly one-layered, locally two-layered, 220–400 μm thick, covered with sparse slime, where two-layered with a distinctly delimited suprapellis sitting on a well-delimited and strongly gelatinized subpellis of narrow hyphae that is abruptly separated from the voluminous sphaerocystes of trama; suprapellis (where two-layered) ± 50 μm thick, composed of pileocystidia and chains of 3–5 fusiform, clavate or cylindrical septate cells 4–10 (12) μm wide, the terminal cells up to 20 μm long, subclavate, cylindrical or slighly tapering; pileocystidia common to numerous, often aggregate into piles, 13–53 × 4–8 μm, fusiform, sublanceolate, often mucronate or with a central knob at the apex, with granular, crystalline or amorphous contents, nearly colourless, changing to greyish black or blackish brown in SV; subpellis (or whole pileipellis where one-layered) a loose tissue of very narrow hyphae lacking pileocystidia, 200–400 μm thick, hyphae 2–4 μm wide, often branching, strongly shrivelled, with clear outline in a gelatinized matrix, becoming repent and slightly wider (3–6 μm) towards pileus trama, at the very bottom and adjacent trama with scattered to moderately numerous cylindrical cystidioid hyphae 100–200 × 7–12 μm, those with strongly refractive crystalline contents turning to greyish black in SV. Stipitipellis one-layered, 10–55 μm thick, locally with repent or erect caulocystidia; caulocystidia common, 16–50 × 5–8 μm, subfusiform, subcylindrical, with crystalline contents turning to greyish black in SV. Pileus and stipe trama with numerous rosettes and connective hyphae; sphaerocystes 13–70 μm in diam, connective hyphae 3–8 μm wide, oleiferous hyphae common, with granular or amorphous contents. Clamp connections absent.

Additional specimens examined China, Yunnan Prov., Wenshan Pref., Maguan Co., Dalishu Town, Xiangchang, 23°04′09″ N, 104°12′33″ E, 1650–1690 m asl, 14 Oct. 2017, leg. X.H. Wang, no. 4767 (HKAS 102279, KUN), no. 4749 (HKAS 102276, KUN); ibid., 14 Oct. 2017, leg. J. Wang, no. 292 (HKAS 102275); Maguan Co., Mabai Town, Yubo, 23°00′57.9″ N, 104°20′59.5″ E, 1364 m asl, 15 Oct. 2017, leg. X.H. Wang, no. 4785 (HKAS 102280, KUN).

Habit, habitat and distribution Scattered, during fall, in mixed forest of fagaceous trees and *Pinus kesiya* var. *langbianensis*. Subtropical China and Japan (Mie, Yakushima Island).

Notes: The pileus of *R. substriata* is not as brightly coloured and lilac red as *R. maguanensis*, although in one specimen (HKAS 102276, Fig. 3d), the colour is close. The lamellae of *R. substriata* seem to be not as brittle as those of *R. maguanensis*, but this difference needs more testing with additional specimens of *R. maguanensis*. The spores of *R. substriata* are slightly longer than those of *R. maguanensis*. Absence of greenish tinge can easily distinguish these two new species from Indian *R. shingbaensis* and Chinese *R. verrucospora* (Das et al. 2014; Song et al. 2018b). The lamellulae of *R. substriata* are more frequent than those of *R. maguanensis* and *R. shingbaensis* (Das et al. 2014), but comparable with or fewer than in *R. verrucospora*. *Russula verrucospora* has the smallest spores (av. 5.7 × 5.0 μm) among the four Asian species.

Although *R. substriata* is here described as a new species, its mycorrhizae have been reported several times in Asia. In China, it was found in mixed forest of *Pseudotsuga sinensis* and *Pinus* spp. in Hunan, central China (as "*Russula* sp.12", Wen et al. 2015), in mixed forest of *Pinus massoniana* and fagaceous trees in Zhejiang, eastern China (GenBank accession JQ991798) and in *Castanopsis fargesii* forest in Sichuan, southwestern China (Wang et al. 2011 and GenBank accessions JF273535 and JF273556). Matsuda et al. (2011) found that it was associated with *Monotropastrum humile* in

oak forest in central Japan (Mie). It is one of the most common *Russula* species in Maguan County, Yunnan. We notice that *R. substriata* co-occurs with *R. maguanensis* both in Maguan, China and Yakushima island, Japan (Fig. 2). How two closely related species evolved sympatrically and dispersed would be an intriguing biogeographical topic.

Russula subsect. *Substriatinae* X.H. Wang & Buyck, subsect. nov.

MycoBank: MB 828233.

Type species: *Russula substriata* J. Wang, X.H. Wang, Buyck & T. Bau.

Diagnosis: Pileus sticky, tuberculate-striate or nearly so, greenish, olive, greyish rose or lilac red; lamellulae few to frequent, taste mostly mild, rarely acrid, brittle, rarely buttery; spores with isolated warts; hymenial gloeocystidia frequent, fusiform, contents SV+; pileipellis orthochromatic in Cresyl blue, two-layered, suprapellis composed of numerous to abundant pileocystidia and erect septate fusiform terminal cells, pileocystidia with contents SV+, subpellis a loose tissue of very narrow hyphae in a gelatinized matrix, lacking pileocystidia; cystidioid hyphae scattered to common at the bottom of subpellis and pileus trama, with contents SV+.

Species included: *R. substriata*, *R. maguanensis*, *R. shingbaensis* and four potential species from America, Australia and tropical Asia, possibly also *R. verrucospora.*

Discussion

The only described species that is closely related to our two new species for the moment is *R. shingbaensis*, a species recently discovered from Himalayan India, which is across the Chinese border with Tibet (Das et al. 2014). When considering also environmental ITS sequences, we find out that both our species and *R. shingbaensis* are part of a strongly supported larger clade (clade A, Fig. 2) with a distribution that encompasses not only China and India, but also Japan, the southern USA and Mexico and Australia. There are at least seven species in this clade, each occupying one particular continent and in general associated with such diverse hosts as Australian Eucalypts (Myrtacae), American and Asian Fagaceae and Pinaceae, as well as Juglandaceae in Mexico (Bastias et al. 2006; Wang et al. 2011; Das et al. 2014; Wen et al. 2015; data retrieved from Genbank). Moreover, our analysis of environmental sequences suggests that in Australia and Japan, species in this clade are subject to exploitation by heterotrophic plants to get access to the carbon produced by their host plants, and this both by orchids (*Erythorchis cassythoides* in Australian eucalypt stands) and ericaceous plants (*Monotropastrum humile* in Japanese oak stand) (Dearnaley 2006; Matsuda et al. 2011). This assemblage seems to be good representatives in ectomycorrhizal communities.

The widely distributed assemblage above, however, was never recognised as a distinct infrageneric entity in *R.* subg. *Heterophyllidia.* Using ITS data, Das et al. (2014) placed *R. shingbaensis* in *R.* subg. *Heterophyllidia* but could not give further assignment. Also using ITS data but a wider taxa sampling, Song et al. (2018b) found that *R. shingbaensis* was sister to their new species *R. verrucospora* and then a successive sister to *R.* subsect. *Cyanoxanthinae*, still in *R.* subg. *Heterophyllidia*. Song et al. (2018b) suggested that *R. verrucospora* might have affinity to tropical African *R.* subsect. *Aureotactinae*, but did not assign it to either *Cyanoxanthinae* or *Aureotactinae* due to clear morphological differences. To test the relationship with *R.* subsect. *Aureotactinae*, we included four sequences of *R.* cf. *brunneoannulata*. Our ITS phylogeny (Fig. 2) suggests that the big assemblage above (including *R. shingbaensis*), *R. verrucospora*, *R.* cf. *brunneoannulata* and *R.* subsect. *Cyanoxanthinae* fell into the same clade, although without significant support. Our 28S-*rpb2-tef1* phylogeny confirmed the sibling relationship between our two species (implicitly also *R. shingbaensis*) and a Malagasy species close to African mainland *R. brunneoannulata* [*R.* aff. *brunneoannulata* in Buyck et al. 2018] and clearly suggested they represented one of the four major clades of *R.* subg. *Heterophyllidia* (Fig. 2).

Following our 28S-*rpb2-tef1* phylogeny, the multi-gene phylogeny of Buyck et al. (2018) and Looney et al. (2016) and hierarchical classification, it is reasonable to split *R.* subg. *Heterophyllidia* into four sections, corresponding to the four major clades A–D (Fig. 1). In such a classification, *R.* subsect. *Substriatinae* and *R.* subsect. *Aureotactinae* compose one of the four sections (clade B), whereas the remaining three correspond to *R.* sect. *Heterophyllae* (clade A), *R.* sect. *Ingratae* (clade C) and *R.* subsect. *Cyanoxanthinae* (clade D). Morphologically, *R.* subsect. *Substriatinae* does share spores with isolated warts and pileipellis with numerous pileocystidia with its sister group *R.* subsect. *Aureotactinae.* However, it clearly differs from all African/Malagasy species of *R.* subsect. *Aureotactinae* in lacking the intense yellowing of surface and context of their fruiting bodies (see Buyck 1994). In addition, the distribution patterns of pileal cystidioid elements are different between the two groups: in *R.* subsect. *Substriatinae*, typical fusiform pileocystidia are only at the outermost surface, i.e. suprapellis, clearly separated from the long cylindrical cystidioid hyhpae at the bottom of subpellis and trama by the thick loose cystidia-free subpellis, whereas in *R.* subsect. *Aureotatinae*, as well as in *R.* sect. *Ingratae*, *R.* subsect. *Cyanoxanthinae* and most species of *R.* sect. *Heterophyllae*, there is a gradual transition from short sometimes mucronate at the surface to longer cylindrical with a blunt apex when going down to the trama (Buyck 1990; Wang et al. 2018). Such clear separation of pileal cystidioid elements is reminiscent of *R. crustosa* complex, which has

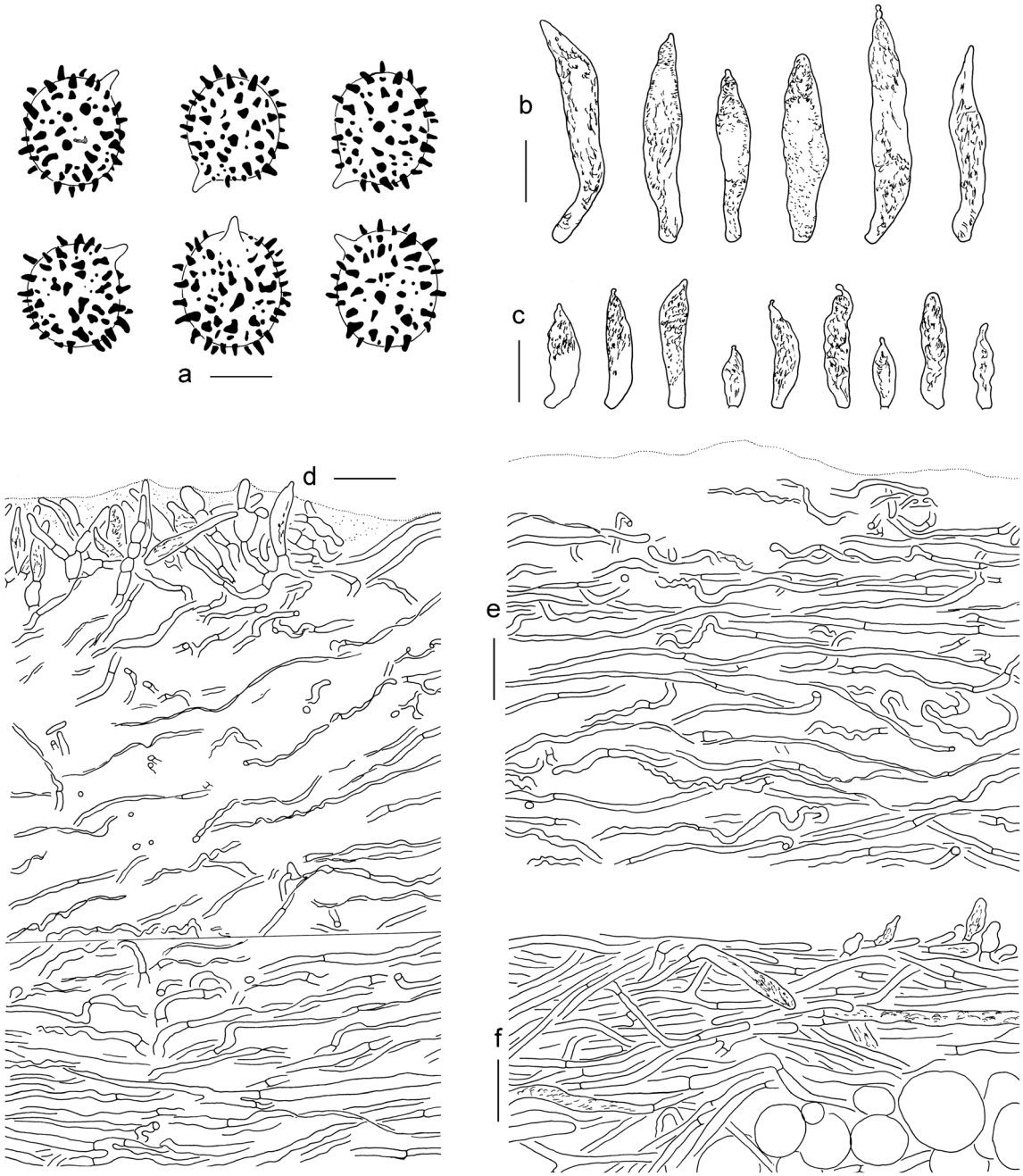

Fig. 5 *Russula substriata* (HKAS 102278, holotype). **a** Basidiospores. **b** Gloeocystidia on gill sides. **c** Gloeocystidia on gill edges. **d** Two-layered pileipellis with aggregate pileocystidia. **e** One-layered pileipellis without pileocystidia. **f** Stipitipellis. Bars: **a** 5 μm; **b**, **c** 20 μm, **d**–**f** 25 μm

subreticulate spores and is distantly placed in *R.* subsect. *Virescentinae* in clade A. In fact, the overall characters of *R.* subsect. *Substriatinae* look very much like a mixture up of all other sections of *R.* subg. *Heterophyllidia*, e.g. the tuberculate-striate pileus margin and the multi-chambered stipe cortex of some specimens are strongly reminiscent of *R.* sect. *Ingratae*, the short-celled branching hyphal endings in the pileipellis of *R.* subsection *Griseinae*, the finely cracked pileus cuticle (at least in *R. maguanensis* and *R. substriata*) of *R. crustosa* group (*R.* subsect. *Virescentinae*) and spores with isolated warts of some species of *R.* sect. *Heterophyllae*. Recognising this assemblage as an infrageneric subdivision will be of importance to highlight the diverse combinations of morphological characters within *Russula.*

After *R.* subsect. *Substriatinae* is described in *R.* subg. *Heterophyllidia*, two questions will be left: (1) what is the section for subsections *Substriatinae* and *Aureotactinae*? Unfortunately, there is no available valid section name for them. There are two candidate names, i.e. *R.* sect. *Aureotactae* and *R.* sect. *Radicantes* (Fig. 5). However, neither

is valid (Buyck 1990). Nevertheless, we feel it is premature to validate the name in this study because the type species from Madagascar, *R. aureotacta* R. Heim and *R. radicans* R. Heim have never been found again since their description and no sequences are available to verify their true affinities to our representative of *R.* subsect. *Aureotactinae.* Moreover, the possibility that subsections *Substriatinae* and *Aureotactinae* may merit two independent sections cannot be easily excluded. Genetically, even in the phylogeny constructed with three conservative loci (with introns and ambiguous sites removed), the branches leading to subsections *Substriatinae* and *Aureotactinae* both are very long, in sharp contrast to the short branch grouping them together and the support values are relatively low in the ML analysis (ML-BP 71%) in comparison with other three equivalent lineages. In the ITS genealogy, the monophyletic relationship of the two subsections could even not be re-trieved (Fig. 2). (2) Does *R. verrucospora* belong to *R.* subsect. *Substriatinae*? Although Song et al. (2018b) grouped *R. verrucospora* with *R. shingbaensis* with high support, the sibling relationship of *R. verrucospora* and our new subsection in the ITS genealogy did not receive significant support. On top of this, the extremely small spores with typical round rather than conical or truncate warts, the presence of pileocystidia in the subpellis and the obscurely striate pileus of *R. verrucospora* make this species not fully fulfil the morphological criterion of *R.* subsect. *Substriatinae.* We leave these two questions as open until more representatives of "*R.* sect. *Aureotactae*" and our new subsection are sequenced and multi-gene data are available for *R. verrucospora* and its potential allies, to avoid any possible artfact in phylogenetic analyses (e.g. long branch attraction). This study as well addresses nomenclatural issue regarding *R.* subsect. *Cyanoxanthinae* as it merits a section in this updated classification. We leave it for a thorough update of infrageneric classification of *Russula* with a broader sampling.

Funding information This study is funded by the CAS Key Laboratory for Plant Diversity and Biogeography of East Asia, Kunming Institute of Botany, Chinese Academy of Sciences (project no. LPB201501) and the project "Investigation of Macrofungi of Maguan County" issued by Ministry of Ecology and Environment of the People's Republic of China to XHW.

References

Ariyawansa HA, Hyde KD, Jayasiri SC, Buyck B, Chethana KWT et al (2015) Fungal diversity notes 111–252 — taxonomic and phylogenetic contributions to fungal taxa. Fungal Divers 75:27–274

Bastias B, Xu ZH, Cairney JWG (2006) Influence of long-term repeated prescribed burning on mycelial communities of ectomycorrhizal fungi. New Phytol 172:149–158

Buyck B (1989) Utilité taxonomique du bleu de crésyldans le genre *Russula* Persoon. Bull Trimest Soc Mycol Fr 95:1–6

Buyck B (1990) Nouveaux taxons infragénériques dans le genre *Russula* Persoon en Afrique centrale. Bull Jard Bot Nat Belg 60:191–211

Buyck B (1994) *Russula* II (Russulaceae). In: Rammeloo J, Heinemann P (eds) Flore illustreé des Champignons d' Afrique Centrale, vol 16, pp 411–542, pl 69–87

Buyck B, Hofstetter V, Eberhardt U, Verbeken A, Kauff F (2008) Walking the thin line between *Russula* and *Lactarius*: the dilemma of *Russula* subsect. *Ochricompactae*. Fungal Divers 28:15–40

Buyck B, Zoller S, Hofstetter V (2018) Walking the thin line…ten years later: the dilemma of above versus below-ground features to support phylogenies in the Russulaceae (Basidiomycota). Fungal Divers 89: 267–292

Das K, Dowie NJ, Li GJ, Miller SL (2014) Two new species of *Russula* (Russulales) from India. Mycosphere 5:612–622

Das K, Ghosh A, Chakraborty D, Li JW, Qiu LH et al (2017) Fungal biodiversity profiles 31-40. Cryptogam Mycol 38:353–406

Dearnaley J (2006) Molecular identification of fungal endophytes in Australian myco-heterotrophic orchids. In: 8th International Mycological Congress (IMC8), 20–25 Aug 2006, Cairns, Australia

Guo J, Karunarathna SC, Mortimer PE, Xu J, Hyde KD (2014) Phylogenetic diversity of *Russula* from Xiaozhongdian, Yunnan, China, inferred from internal transcribed spacer sequence data. Chiang Mai J Sci 41:811–821

Hall TA (1999) BioEdit: a user-friendly biological sequence alignment editor and analysis program for windows 95/98/NT. Nucleic Acids Symp Ser 41:95–98

Hansen K, Perry BA, Dranginis AW, Pfister DH (2013) A phylogeny of the highly diverse cup-fungus family Pyronemataceae (Pezizomycetes, Ascomycota) clarifies relationships and evolution of selected life history traits. Mol Phylogenet Evol 67:311–335

Jiang XM, Li YK, Liang JF, Wu JR (2017a) *Russula brunneovinacea* sp. nov. from northeastern China. Mycotaxon 132:789–797

Jiang XM, Li YK, Liang JF, Wu JR (2017b) Two new *Russula* species in China. Journal of Fujian Agriculture and Forestry University (Natural Science Edition) 46:103–108

Katoh K, Toh H (2008) Recent developments in the MAFFT multiple sequence alignment program. Brief Bioinform 9:286–298

Kornerup A, Wanscher JH (1961) Farver i Farver. Politikens Forlag, København

Li F, Deng QL (2018) Three new species of *Russula* from South China. Mycol Prog 17:1305–1321

Li GJ, Li SF, Wen HA (2011) *Russula zhejiangensis* sp. nov. from East China. Cryptogam Mycol 32:127–123

Li GJ, Zhao D, Li SF, Yang HJ, Wen HA, Liu XZ (2012) *Russula jilinensis* sp. nov. (Russulaceae) from Northeast China. Mycotaxon 120:49–58

Li GJ, Zhao Q, Zhao D, Yue SF, Li SF, Wen HA, Liu XZ (2013a) *Russula atroaeruginea* and *R. sichuanensis* spp. nov. from Southwest China. Mycotaxon 124:173–188

Li GJ, Zhao D, Li SF, Yang HJ, Wen HA, Liu XZ (2013b) *Russula changbaiensis* sp. nov from Northeast China. Mycotaxon 124: 269–278

Li YK, Zhang X, Yuan Y, Cao Z, Liang JF (2015a) Morphological and molecular evidence for a new species of *Russula* (Russulaceae) from southern China. Phytotaxa 202:94–102

Li GJ, Zhao D, Li SF, Wen HA (2015b) *Russula chiui* and *R. pseudopectinatoides,* two new species from southwestern China supported by morphological and molecular evidence. Mycol Prog 14(6):33

Li GJ, Zhang CL, Lin FC, Zhao RL (2018a) Hypogeous gasteroid *Lactarius sulphosmus* sp. nov. and agaricoid *Russula vinosobrunneola* sp. nov. (Russulaceae) from China. Mycosphere 9:838–858

Li GJ, Zhang CL, Zhao RL, Lin FC (2018b) Two new species of *Russula* from Northeast China. Mycosphere 9:431–443

Liu YJ, Whelen S, Benjamin DH (1999) Phylogenetic among ascomycetes: evidence from an RNA polymerase II subunit. Mol Biol Evol 16:1799–1808

Liu XL, Bau T, Wang XH (2017) Species diversity of *Russula* from the greater and lesser Hinggan Mountains in Northeast China. Mycosystema 36:1355–1368

Looney BP, Ryberg M, Hampe F, Sánchez-García M, Matheny PB (2016) Into and out of the tropics: global diversification patterns in a hyperdiverse clade of ectomycorrhizal fungi. Mol Ecol 25:630–647

Matsuda Y, Okochi S, Katayama T, Yamada A, Ito S-I (2011) Mycorrhizal fungi associated with *Monotropastrum humile* (Ericaceae) in central Japan. Mycorrhiza 21:569–576

Moncalvo JM, Lutzoni F, Rehner SA, Jhonson J, Vilgalys R (2000) Phylogenetic relationships of agaric fungi based on nuclear large subunit ribosomal DNA sequences. Syst Biol 49:278–305

Nylander JAA (2004) MrModeltest 2.3. Program distributed by the author. Evolutionary Biology Center, Uppsala University

Rambaut A, Drummond AJ, Xie D, Baele G, Suchard MA (2018) Posterior summarisation in Bayesian phylogenetics using tracer 1.7. Syst Biol 67:901–904

Rehner SA, Buckley E (2005) A *Beauveria* phylogeny inferred from nuclear ITS and EF1-a sequences: evidence for cryptic diversification and links to *Cordyceps* teleomorphs. Mycologia 97:84–98

Ronquist F, Teslenko M, van der Mark P, Ayres DL, Darling A et al (2012) MrBayes 3.2: efficient bayesian phylogenetic inference and model choice across a large model space. Syst Biol 61:539–542

Sang XY, Li XD, Wang YW, Fan L (2016) Four new sequestrate species of Russulaceae found in China. Phytotaxa 289:101–117

Singer R (1962) The Agaricales in modern taxonomy. 2nd Edition. J. Cramer, Weinheim

Song B, Li TH, Wu XL, Li JJ, Shen YH, Lin QY (2007) Known species of *Russula* from China and their distribution. Journal of Fungal Research 5:20–42

Song Y, Buyck B, Li JW, Yuan F, Zhang ZW, Qiu LH (2018a) Two novel and a forgotten *Russula* species in sect. *Ingratae* (Russulales) from Dinghushan Biosphere Reserve in southern China. Cryptogam Mycol 39:341–357

Song Y, Li J, Buyck B, Zheng J, Qiu LH (2018b) *Russula verrucospora* sp. nov. and *R. xanthovirens* sp. nov. two novel species of *Russula* (Russulaceae) from southern China. Cryptogam Mycol 39:129–142

Stamatakis A (2006) RAxML-VI-HPC: maximum likelihood-based phylogenetic analyses with thousands of taxa and mixed models. Bioinformatics 22:2688–2690

Tibpromma S, Hyde KD, Jeewon R, Maharachchikumbura SSN, Liu JK et al (2017) Fungal diversity notes 491–602: taxonomic and phylogenetic contributions to fungal taxa. Fungal Divers 83:1–261

Vilgalys R, Hester M (1990) Rapid genetic identification and mapping of enzymatically amplified ribosomal DNA from several *Cryptococcus* species. J Bacteriol 172:4238–4246

Wang XH, Yang ZL, Li YC, Knudsen H, Liu PG (2009) *Russula griseocarnosa* sp. nov. (Russulaceae, Russulales), a commercially important edible mushroom in tropical China: mycorrhiza, phylogenetic position, and taxonomy. Nova Hedwigia 88:269–282

Wang Q, Gao C, Guo LD (2011) Ectomycorrhizae associated with *Castanopsis fargesii* (Fagaceae) in a subtropical forest, China. Mycol Prog 10:323–332

Wang XH, Buyck B, Verbeken A, Hansen K (2015) Revisiting the morphology and phylogeny of *Lactifluus* with three new lineages from southern China. Mycologia 107:941–958

Wang XH, Das K, Horman J, Antonin V, Baghela A et al (2018) Fungal biodiversity profiles 51-60. Cryptogam Mycol 39(2):1–47

Wen ZG, Murata M, Xu ZY, Chen YH, Nara K (2015) Ectomycorrhizal fungal communities on the endangered Chinese Douglas-fir (*Pseudotsuga sinensis*) indicating regional fungal sharing overrides host conservatism across geographical regions. Plant Soil 387:189–199

White TJ, Bruns T, Lee S, Taylor J (1990) Amplification and direct sequencing of fungal ribosomal RNA genes for phylogenetics. In: Innis MA, Gelfand DH, Sninsky JJ, White TJ, editors. PCR protocols. A guide to methods and applications. San Diego, Academic, pp. 315–322

Yin JH, Zhang P, Gong QF, Chen ZH (2008) Sequence analysis of the internal transcribed spacer of gene coding for rDNA in *Russula subnigricans* and *R. nigricans*. Mycosystema 27:237–242

Zhang JB, Li JW, Li F, Qiu LH (2017) *Russula dinghuensis* sp. nov. and *R. subpallidirosea* sp. nov., two new species from southern China supported by morphological and molecular evidence. Cryptogam Mycol 38:191–203

Zhao Q, Li YK, Zhu XT, Zhao YC, Liang JF (2015) *Russula nigrovirens* sp. nov. (Russulaceae) from southwestern China. Phytotaxa 236: 249–256